Optics and Lasers in Engineering 103 (2018) 46–54

Contents lists available at ScienceDirect

Optics and Lasers in Engineering

journal homepage: www.elsevier.com/locate/optlaseng

Full-parallax 3D display from stereo-hybrid 3D camera system

Seokmin Hong*, Amir Ansari, Genaro Saavedra, Manuel Martinez-Corral

University of Valencia, 3D Imaging and Display Laboratory, Department of Optics, Burjassot, Valencia, E-46100, Spain

ARTICLE INFO

Keywords:
3D display
Integral imaging
3D data registration
Color transfer
Point cloud
Stereo-hybrid 3D camera

ABSTRACT

In this paper, we propose an innovative approach for the production of the microimages ready to display onto an integral-imaging monitor. Our main contribution is using a stereo-hybrid 3D camera system, which is used for picking up a 3D data pair and composing a denser point cloud. However, there is an intrinsic difficulty in the fact that hybrid sensors have dissimilarities and therefore should be equalized. Handled data facilitate to generating an integral image after projecting computationally the information through a virtual pinhole array. We illustrate this procedure with some imaging experiments that provide microimages with enhanced quality. After projection of such microimages onto the integral-imaging monitor, 3D images are produced with great parallax and viewing angle.

1. Introduction

During the last century, the three-dimensional (3-D) imaging systems have been issued in order to record and display 3-D scenes. Among them, integral-imaging (InI) has been considered as one of the prospective technologies in order to reflect real 3-D scenes into a multi-visual display system. This concept was proposed by G. Lippmann in 1908. He presented the possibility of capturing the 3-D information and reconstructing the 3-D scene by using spherical diopter arrays [1–3]. Depending on its manipulation, InI is classified by two stages: pickup and display. Nowadays, the pickup procedure is performed by placing a tiny lens array in front of a two-dimensional (2-D) imaging sensor and producing the collection of microimages. A noteworthy feature is that every microimage contains different perspective information. This is because all of the light rays reflected (or diffused) by an object are transmitted by all the lenses, which distribute the light on different pixels of the microimages depending on the incidence angle. Hereafter, the whole array of microimages is referred to as the integral image. Concerning the display stage, when the integral image is projected onto an InI display system, observers can see the 3-D floating color scene, which has full-parallax and quasi-continuous perspective view [4–7]. Many researchers and companies have applied the InI technique in many different fields [8–18].

In the meantime, various depth-sensing techniques were launched in order to record 3-D scenes [19–25]. Among all, one of highlighted techniques is stereovision, which takes advantage of the disparity information from two aligned cameras which has been the representative of the depth-image sensing for a long period [19–20]. Incidentally, in the past decades, the use of technologies related to infrared (IR) light sensors has become spotlighted [21–25]. Especially the Kinect device from Microsoft takes profit from IR lighting technology in the case of depth acquisition. By this time, two different versions of the Kinect are released. The main commercial specifications of Kinect v1 (Kv1) and v2 (Kv2) are described in Table 1. These devices allow to acquire RGB images, IR images and also depth information in real-time with a high frame rate. As well known, both devices have many different features for obtaining a dense depth map. Kv1 uses a structured IR light pattern emitter and IR camera to calculate the depth distance through the captured pattern [21–23]. In contrast, Kv2 utilizes time-of-flight (ToF) technology, which exploits emitting IR beams with high frequency. Having the reflected IR light from most 3-D surfaces, the sensor evaluates the depth distance by measuring the IR flash's returning duration [24–25].

In a previous work, we proposed the use of RGB image and depth information obtained by a single 3-D camera to generate an integral image and project it onto an InI display system [13–15]. However, this innovative approach still contains several issues that must be improved. Among them, the main drawbacks are domination of the depth information by the noise caused by the limitation of IR light sensing technique; the low density of depth map, which is restricted by the sensor's specification; and the depth-hole problem, which occurs because of the reflections and/or occlusions. Mono-perspective devices can see only the frontal part of scenes, so that occluded area's information is lost in the scene.

* Corresponding author.
E-mail address: seokmin.hong@uv.es (S. Hong).

https://doi.org/10.1016/j.optlaseng.2017.11.010
Received 21 June 2017; Received in revised form 19 October 2017; Accepted 13 November 2017

Table 1
Comparison between Kv1 and Kv2 specifications.

List	Kinect v1	Kinect v2
Released (year)	2010	2014
RGB camera (pixel)	640 × 480 (Max: 1280 × 960)	1920 × 1080
Frames per second in RGB camera	30 (Max: 12)	30 (low-light condition: 15)
IR camera (pixel)	640 × 480	512 × 424
Frames per second in IR camera	30	30
Depth acquisition method	Structured IR light pattern	Time of Flight
Suitable depth range (mm)	800–4000	500–4500
IR camera's Horizontal FOV (°)	57	70
IR camera's Vertical FOV (°)	43	60

Table 2
Calibrated camera parameters to calculate the scale factor between target sensors.

Sensor	Coordinate (u: width, v: height)	Resolution (# of pixels)	Sensor size (mm)	Pixels per mm	Focal length (mm)
Kinect v1 (RGB camera)	u	640	3.58	178.771	3.099
	v	480	2.87	167.247	
Kinect v2 (IR camera)	u	512	5.12	100	3.657
	v	424	4.24	100	

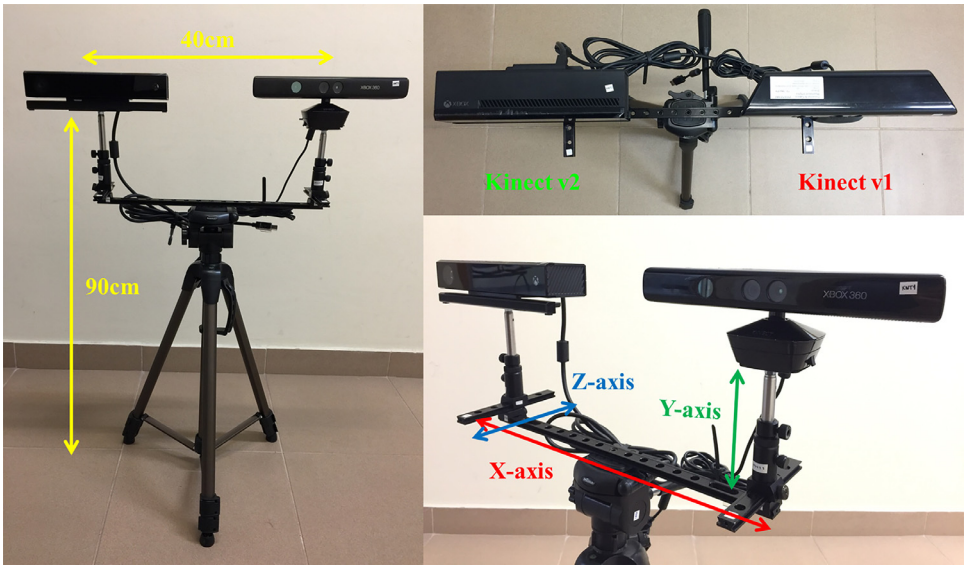

Fig. 1. Proposed stereo-hybrid 3-D camera system.

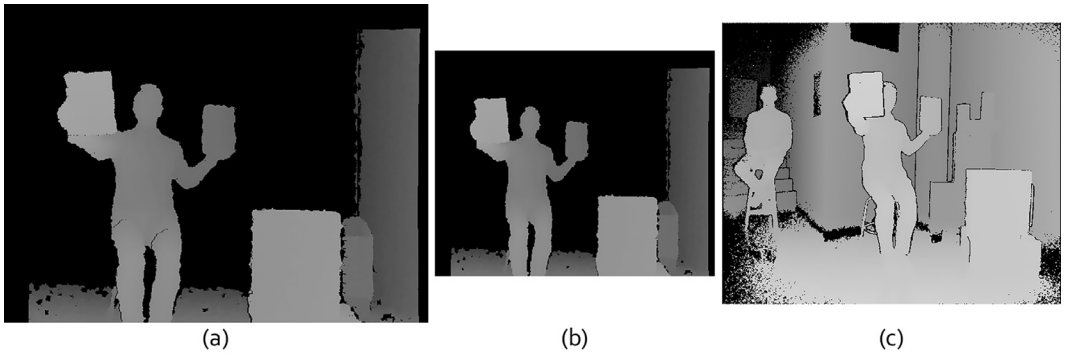

Fig. 2. Captured depth maps from our experimental camera system: (a) from Kv1, (b) rescaled image; and (c) from Kv2.

In order to solve these limitations, we propose the use of stereo-hybrid 3-D camera system. Fig. 1 shows our camera setting. In comparison to monocular system, stereo-vision system can generally extend the field of view (FOV) against with. In order words, our approach can expand the visual space and obtain the occluded information taking advantage of binocular system. Thus, depth-hole area is filled in by complementing each other. Another important advantage of the proposed method is yielding denser point cloud. This procedure is described in Section 2. With this improved 3-D data, the microimages are generated with higher quality. The microimages generation process is described

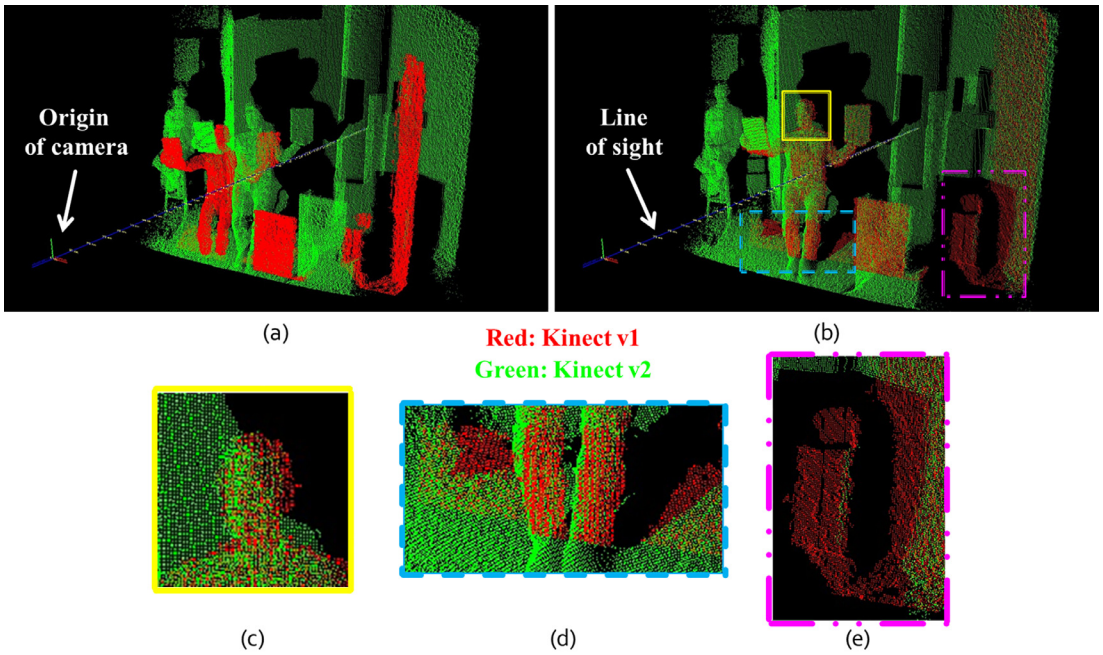

Fig. 3. 3-D point clouds in the virtual 3-D space: (a) before registration process; (b) after calculation result; in (c–e) we magnified some specific parts of the scene. In the figures, red color point is rescaled point clouds from Kv1, and green color point is from Kv2 respectively. (For interpretation of the references to color in this figure legend, the reader is referred to the web version of this article.)

in Section 3. Finally, in Sections 4 and 5 we provide our experimental results and conduct the conclusions respectively.

2. Stereo-Hybrid point clouds manipulation

In order to implement the stereo system, it is convenient either the use of two 3-D cameras of the same model, or the use of two different 3-D cameras with complementary features. In our approach we have decided to make use of Kinect technology. To the best of our knowledge, high frame rate synchronization of two Kv2 nor two Kv1 is never addressed so far. Hence at this stage of our research we have decided to tackle the implementation of a stereo-hybrid technique by taking profit of complementary features of Kv1 and Kv2. Note that even in the case of 2-D cameras, it has been very unusual to compose hybrid camera systems [26–28]. This is an evident motivation why we want to use hybrid 3-D cameras into our research, since its outcomes can be very useful for a potential manipulation of various types of cameras in further research. In the Section 2.1, the correction of the different scale information between sensors will be explained. In sequence, the arrangement and registration of the individual 3-D point cloud information will be shown. In Section 2.2, the correction of the color dissimilarity of sensors will be presented.

2.1. Hybrid point clouds registration

In our previous paper [15], we mentioned about the difference between Kv1 and Kv2. Above all, each Kinect devices has two camera sensors (RGB and IR) by its own, and the four sensors have different FOV and image resolution. It means that all of them have their own scale factors, which need to be corrected. In [26], authors proposed how to correct the scale information in hybrid stereoscopic 2-D camera systems. The algorithm manages the images captured by two different sensors, the input image and the target image, and aims to obtain a rescaled input image. Eqs. (1) and (2) show how to derive scale factors: $i_{u,\,v}$ refers to number of pixels in the input image, while $j_{u,\,v}$ is the number of pixels in the corrected input image. Besides, f, f' are input and target focal lengths (mm), whereas $p_{u,\,v}$, $p'_{u,v}$ are input and target pixels/mm.

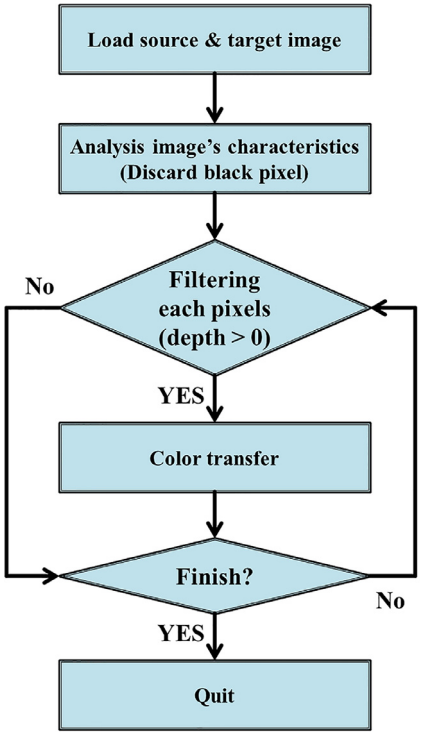

Fig. 4. Flow chart of the proposed color transferring strategy. The loop is applied voxel by voxel.

$$\begin{cases} j_u = \dfrac{i_u f' p'_u}{f p_u} = \lambda_u i_u \\ j_v = \dfrac{i_v f' p'_v}{f p_v} = \lambda_v i_v \end{cases} \tag{1}$$

Fig. 5. Processed result by using referenced color transfer algorithm (a) rescaled RGB image captured by Kv1 (b) the captured RGB image from Kv2 (c) color transferred result from (b) to (a).

Fig. 6. Orthographic projection of registered 3-D point cloud: (a) before color transferring process (b) is after color transfer. Note that (b) shows more natural textured scene than (a).At the scene, the black pixels have no information because they are out of the depth-range capacity of IR sensing.

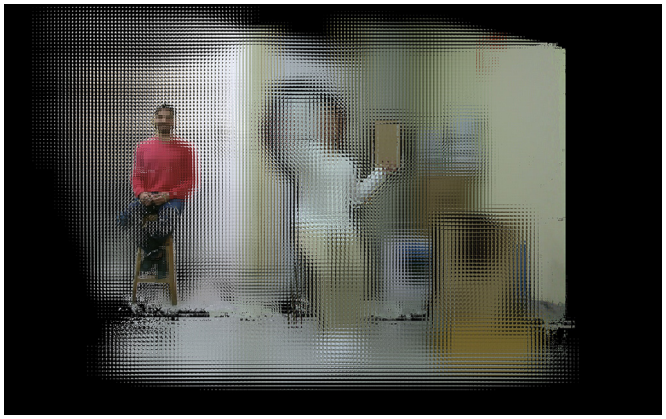

Fig. 7. Collection of microimages generated from modified 3-D point cloud. In this case, the reference plane is placed in 2450 mm distance from the origin of Kv2.

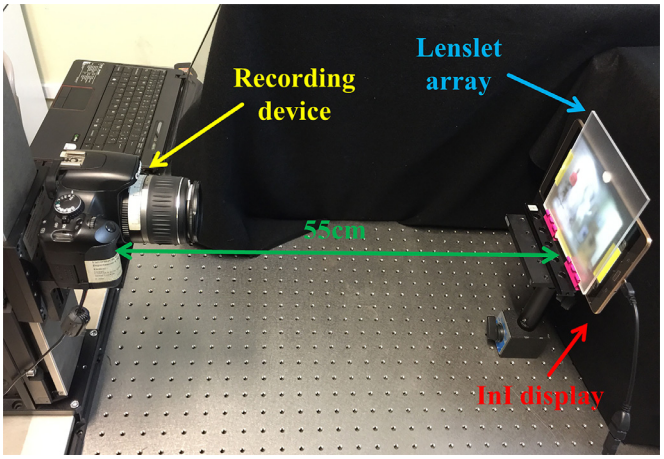

Fig. 8. Overview of experimental system.

Where we have defined parameter

$$\lambda_{u,v} = \frac{f' p'_{u,v}}{f p_{u,v}} \tag{2}$$

as the scale factor between target and input sensors.

In our approach, input image is Kv1's RGB image and target image is Kv2's IR image. There are several reasons why we decided to transpose from Kv1's RGB camera to Kv2's IR camera. First, mapping from IR image to RGB image in Kv1 is feasible because of many solutions are already released. Second, Kv2 depth information is denser and with larger FOV than Kv1. Finally, the third reason is that in the Kv2, the resolution in RGB camera is much bigger than that in IR camera. If we would map from IR image to RGB image, in Kv2, IR image needs, not only to up-scaling, but also interpolate the pixel gaps in rescaled image.

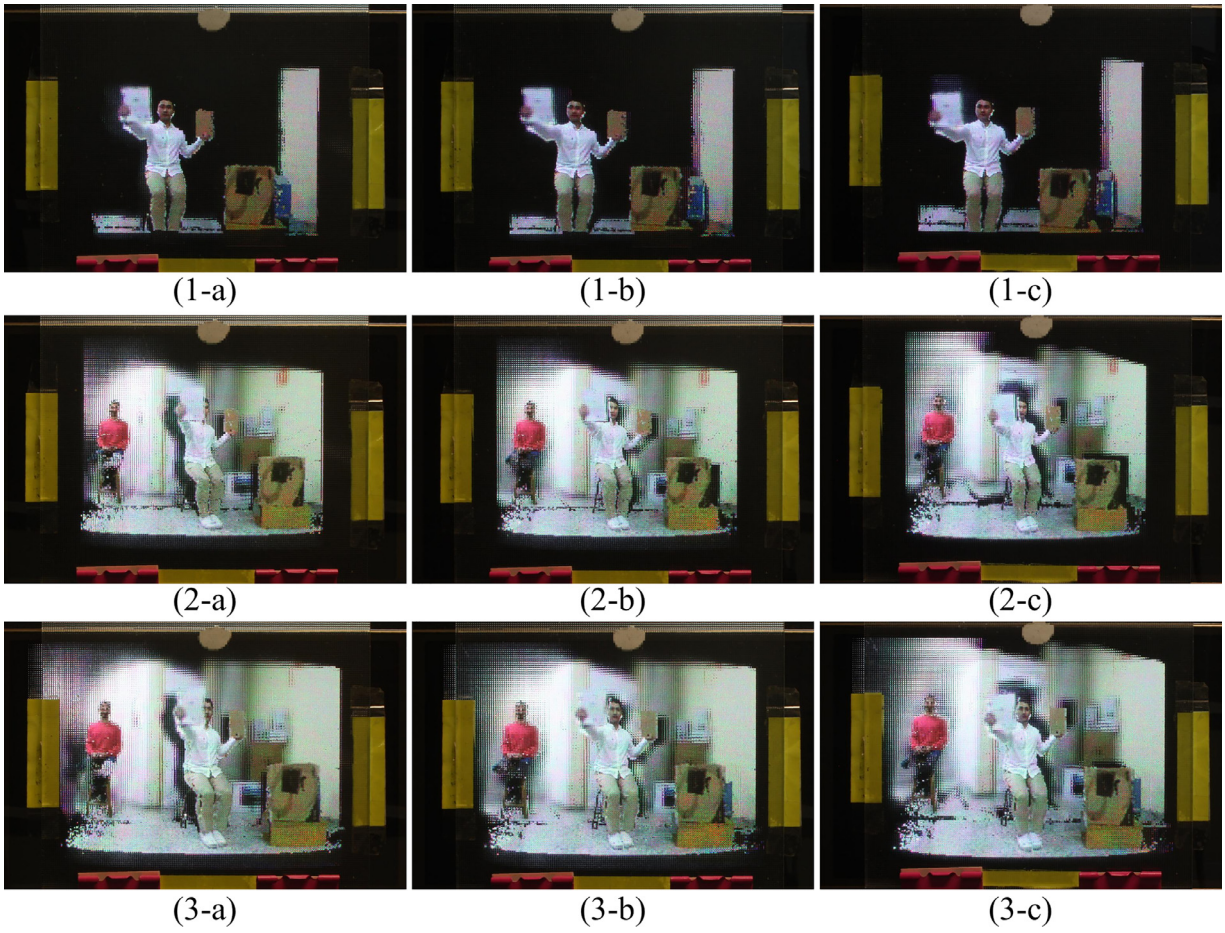

Fig. 9. Comparison result between displayed integral image: (1-a, b, c) Kv1, (2-a, b, c) Kv2, (3-a, b, c) the proposed result. (a, b, c) shows different perspective position where (a) is left-bottom, (b) is right-bottom, and (c) is right-top from the InI monitor. All images are excerpted from recorded video: media 2, 3, and 4.

Fig. 10. More detail comparison of displayed integral image. This figure shows the advantage of our approach. We filled in several depth-hole areas and derived to smoother texture at the scene. Above all, some occluded area is recovered precisely.

To calculate the scale factor, the well-treated data from [29] is followed, where both Kinect parameters were calibrated accurately (see Table 2). Then the scale factors are, $\lambda_u = 0.660$, $\lambda_v = 0.706$; and rescaled input resolutions are $j_u \cong 422.46$, $j_v \cong 338.68$. Fig. 2 shows captured depth map from Kv1 and Kv2's IR sensors and rescaled result. See the figures for further details.

From now on, rescaled image resolution of Kv1's RGB and Kv2's IR camera are adapted to the same scale information. Afterward, the captured RGB and Depth information from each device can compose point cloud and dispose into a virtual 3-D space. However, both cloud data are still mutually shifted and not arranged properly (See Fig. 3(a)). In order to make registration between two point cloud sets, Iterative-Closest-Point (ICP) algorithm is utilized. ICP algorithm calculates the movement between two sets of point clouds in order to minimize their distance. ICP is often used to reconstruct 2-D or 3-D data captured from different positions. The output of ICP algorithm is rigid (or rigid body) transformation matrix, which includes translation and rotation [30–32]. Fig. 3 shows the point cloud before and after registration result. The red and green colors represent the point cloud obtained by Kv1 and Kv2 respectfully. As it can be seen, the Kv1's data are well-aligned into Kv2 and covered in some occluded area. Especially, Fig. 3(c–e) indicates more detail of the registration result clearly.

2.2. Color transfer between color images

Even when the two point clouds are registered properly, the RGB images of the Kv1 and Kv2 still have color dissimilarities. To overcome this drawback, the color transfer method proposed by Reinhard et al. [33] is followed, but it is adapted to 3-D images. Our approach is described in the flowchart of Fig. 4. In the second step, after loading the input and target point clouds, the black voxels having no color information are discarded. Then, the voxels without depth information were filtered out. The reason for such discarding is that those meaningless voxels would transfer wrong color characteristics. As result of applying the algorithm to all the voxels, the Kv2's RGB color values are transferred onto the characteristics of the Kv1's RGB image. Figs. 5 and 6 show the color-transfer result clearly. In Fig. 5(a) we show the input RGB image (obtained with Kv1), in Fig. 5(b) the target RGB image (Kv2) and finally in Fig. 5(c) the modified input image after the color transference.

Fig. 6 shows orthographic projection of RGB information of registered 3-D point clouds. Fig. 6(a) shows the point cloud before the color transfer, while Fig. 6(b) shows the same point cloud after the transfer. In Fig. 6, the areas of the scene where significant improvement is obtained due to the color transfer have been marked. In order to illustrate and demonstrate our proposal, the video Media 1 is composed with this sequence: point clouds of Kv1, Kv2, without registration result, and registration with color transfer result respectively.

3. Microimages generation from point clouds

In order to generate the microimages for their projection onto the InI display system, our previous approach [14] is followed. Then in our algorithm we placed a virtual pinhole array (VPA) at a certain distance from the 3-D point cloud. Indeed, VPA's location reflects the correlation between real scene and displayed scene. In particular, this position determines the front and rear volumes at the displayed 3-D scene. Accordingly, we entitle this position as a reference plane. Then, the voxels of each point cloud are projected through the VPA, so that the integral image is composed, as in [34]. In this back-projection scheme, each microimage records the angular information. In fact, the calculation of the microimages needs to account for the parameters of the InI display system; i.e. the number of microlenses, their pitch, gap, and number of pixels behind any microlens. Fig. 7 shows calculated microimages, which are ready for projection through the InI display.

4. Experimental results of displayed three-dimensional image

In our experiment, the InI monitor is composed of a Samsung SM-T700 (359 pixels/inch) tablet, and a MLA consisting of 181×113 lenslets of focal length $f = 3.3$ mm and pitch $p = 1.0$ mm (Model 630 from Fresnel Technology). Each microimage is composed of 15×15 pixels, the gap between the microlenses and the display is fixed to $g = 49.5$ pixels, and thus, the full size of the integral image is 2715×1695 pixels (14.13 pixels/mm). After mounting and aligning the MLA in front of the tablet, the 3-D scene is displayed with full-parallax.

To demonstrate the proposed approach, the setup is implemented as shown in Fig. 8. The InI monitor displays and integrates the microimages towards the observer's eyes. Originally, our target is binocular observers, who can see the 3-D nature of displayed scene, that is, they can perceive several parts of the displayed scene in front of the monitor and some others behind. Unfortunately, this full-parallax effect cannot be directly demonstrated in a manuscript or even in a monocular video. In order to demonstrate this effect we proceeded as follows. First the observer is replaced by a monocular digital camera. Then a collection of pictures is obtained after displacing horizontally and vertically the camera along a region of 70×70 mm. With these pictures, a video is composed in which the InI monitor was observed from different perspectives. Media 2 and 3 shows Kv1 and Kv2, and Media 4 shows the final modified result. All of the recorded videos are composed of different horizontal and vertical perspective views. The Figs. 9 and 10 show this experimental result more clearly. Modified point clouds are filled in some depth-hole areas and as a result, it induces denser and smoother texture of the scene. The most impressive feature is that some occluded areas are recovered by registration process. Especially, the human model's head and blue basket behind of brown box are recovered properly.

5. Conclusion

To the best of our knowledge, this is the first time to utilize a stereo-hybrid 3-D camera system to capture the light field. Specifically, in order to overcome the limitations of a mono perspective view, the usage of stereo-hybrid system consisting of two Kinect devices is proposed. But we had to tackle the challenge of fusing two different 3-D point clouds with strong dissimilarities: different lateral and axial resolution, different spectral sensitivities of RGB sensors, and even different luminance of the 3-D scene when seen from different perspectives. To cope with these mismatches, some well-known algorithms fitting to our specific situation have been adapted. To demonstrate our approach, a 3-D scene is captured with the stereo-Kinect device and the 3-D point clouds are modified according to our strategy of correcting the dissimilarities. Finally, the improvements in the displayed images have been demonstrated by calculating the microimages and projecting them onto an InI monitor, which provides the observers with full-parallax 3-D images. Since we filled in several depth-hole areas at the integral image and derived to smoother texture at the scene, the experiment confirms that the quality of 3-D data is improved noticeably. Above all, some occluded field is recovered precisely and thus, this output proves the benefit of our manipulation. In a future work, we will apply this technique for different and/or newer types of 3-D cameras: Light-field camera [8–11], and stereo-vision camera [19–20]. In addition, we will enhance the accuracy of 3-D data registration and color equalization result. Finally, we would like to point out that a different experimental concept which is manipulated by LeMaster et al. [35], where they use an array of mid-wave infrared cameras to obtain depth reconstructions for long distances is also complementary as our experiment.

Acknowledgement

This work was supported by the Ministerio de Economía y Competitividad, Spain (Grant no. DPI 2015-66458-C2-1R), and by Generalitat Valenciana, Spain (project PROMETEOII/2014/072). S. Hong acknowledges a predoctoral grant from University of Valencia (UV-INVPREDOC15-265754). And A. Ansari acknowledges a predoctoral contract from EU H2020 program under MSCA grant 676401.

Supplementary materials

Supplementary material associated with this article can be found, in the online version, at doi:10.1016/j.optlaseng.2017.11.010.

References

[1] Lippmann G. Epreuves réversibles photographies integrals. Comptes Rendus de l'Académie des Sciences 1908;146:446–51.
[2] Lippmann G. Epreuves reversibles donnant la sensation du relief. J Phys Théorique et Appl 1908;7:821–5.
[3] Lippmann G. L'étalon international de radium. Radium (Paris) 1912;9:169–70.
[4] Stem A, Javidi B. Three-dimensional image sensing, visualization, and processing using integral imaging. Proc IEEE 2006;94:591–607.
[5] Okano F, Hoshino H, Arai J, Yuyama I. Real-time pickup method for a three-dimensional image based on integral photography. Appl Opt 1997;36:1598–603.
[6] Kim Y, Hong K, Lee B. Recent researched based on integral imaging display method. 3D Res 2010;1:17–27.
[7] Park S, Yeom J, Jeong Y, Chen N, Hong J, Lee B. Recent issues on integral imaging and its applications. J Inf Disp 2014;15:37–46.
[8] Lytro camera, 2011. https://www.lytro.com.
[9] PiCam: Pelican Imaging Camera, 2013. http://www.pelicanimaging.com.
[10] Raytrix camera, 2010. http://www.raytrix.de.
[11] Canesta sensor, 2002. http://en.wikipedia.org/wiki/Canesta.
[12] Ng R, Levoy M, Bredif M, Duval G, Horowiz M, Hanrahan P. Light field photography with a hand-held plenoptic camera. Light field photography with a hand-held plenoptic camera, 2; 2005. Tech. Rep. CSTR. 2.
[13] Hong S, Shin D, Lee J, Lee B. Viewing angle-improved 3D integral imaging display with eye tracking sensor. J Inf Commun Converg Eng 2014;12:208–14.
[14] Hong S, Shin D, Lee B, Dorado A, Saavedra G, Martinez-Corral M. Towards 3D television through fusion of kinect and integral-imaging concepts. J Disp Technol 2015;11:894–9.
[15] Hong S, Saavedra G, Martinez-Corral M. Full parallax three-dimensional display from Kinect v1 and v2. Opt Eng 2016;56:041305.
[16] Dorado A, Saavedra G, Sola-Pikabea J, Martinez-Corral M. Integral imaging monitors with an enlarged viewing angle. J lnf Commun Converg Eng 2015;13:132–8.
[17] Dorado A, Martinez-Corral M, Saavedra G, Hong S. Computation and display of 3D movie from a single integral photography. J Disp Technol 2016;12:695–700.
[18] Han Y, Lee M, Lee B. Air-touch interaction system for integral imaging 3D display. In: First Int. Workshop on Pattern Recognit.; 2016. p. 10011.
[19] Bumblebee2, 2006. http://www.ptgrey.com/stereo-vision-cameras-systems.
[20] ZED, 2015. http://www.stereolabs.com.
[21] Kinect for windows sensor components and specifications; 2013. http://msdn.microsoft.com/en-us/library/jj131033.aspx.
[22] Primesense Calmine 1.08 & 1.09, 2013. http://en.wikipedia.org/wiki/PrimeSense.
[23] ASUS Xtion, 2011. http://www.asus.com/3D-Sensor/Xtion_PRO.
[24] Kinect for Xbox one components and specifications; 2013. http://dev.windows.com/en-us/kinect/hardware.
[25] Intel Realsense, 2014. https://software.intel.com/en-us/realsense.
[26] Shin H, Kim S, Sohn K. Hybrid stereoscopic camera system. J Broadcast Eng 2011;16:602–13.
[27] Garcia F, Aouada D, Mirbach B, Ottersten B. Real-time distance-dependent mapping for a hybrid ToF multi-camera rig. IEEE J Sel Top Signal Process 2012;6:425–36.
[28] Frick A, Koch R. LDV generation from multi-view hybrid image and depth video. In: 3D-TV system with depth-image-based-rendering. New York: Springer; 2012. p. 191–220.

[29] Pagliari D, Pinto L. Calibration of kinect for Xbox one and comparison between the two generations of microsoft sensors. Sensors 2015;15:27569–89.
[30] Besl PJ, Mckay ND. A method for registration of 3-D shapes. IEEE Trans Pattern Anal Mach Intell 1992;14:239–56.
[31] Zhang Z. Iterative point matching for registration of free-form curves and surfaces. Int J Comput Vis 1994;13:119–52.
[32] Rusinkiewicz S, Levoy M. Efficient variants of the ICP algorithm. In: Proceedings Third Int. Conf. on 3-D Digit. Imaging and Mode; 2001. p. 145–52.
[33] Reinhard E, Ashikhmin M, Gooch B, Shirley P. Color transfer between images. IEEE Comput Graph Appl 2001;21:34–41.
[34] Martinez-Corral M, Javidi B, Martinez-Cuenca R, Saavedra G. Formation of real, orthoscopic integral images by smart pixel mapping. Opt Express 2005;13:9175–80.
[35] LeMaster D, Karch B, Javidi B. Mid-wave infrared 3D integral imaging at long range. J Disp Technol 2013;9:545–51.

Seokmin Hong received the B.Eng. and M.Sc. degrees in digital and visual contents from Dongseo University, Busan, South Korea, in 2012 and 2014, respectively. In 2012, Dongseo University honored him with the B.Eng. Extraordinary Award. Since 2015, he has been working with the 3D Imaging and Display Laboratory, Optics Department, University of Valencia, Spain. His research interests are image processing, computer vision, and applied computer science.

Amir Ansari received his master degree in Electrical Engineering-Communication systems from Shiraz University of Technology, Iran in 2014. As a master student, he studied signal/image processing, digital watermarking, image and video coding and his research activity was mainly deviated to hyperscectral image fusion. He also has experience of designing GPS-based remote positioning and telemetry systems. On September 2016, he qualified for Marie Sklodowska Curie scholarship and joined 3DID where he is currently doing his PhD. His research interests include (but are not limited to) image processing/watermarking/fusion, hardware design and navigation systems.

Genaro Saavedra received the B.Sc. and Ph.D. degrees in physics from Universitat de València, Spain, in 1990 and 1996, respectively. His Ph. D. work was honored with the Ph.D. Extraordinary Award. He is currently Full Professor with Universitat de València, Spain. Since 1999, he has been working with the "3D Display and Imaging Laboratory", at the Optics Department. His current research interests are optical diffraction, integral imaging, 3D high-resolution optical microscopy and phase-space representation of scalar optical fields. He has published on these topics about 50 technical articles in major journals and 3 chapters in scientific books. He has published over 50 conference proceedings, including 10 invited presentations.

Manuel Martínez-Corral was born in Spain in 1962. He received the M.Sc. and Ph.D. degrees in physics from the University of Valencia, Spain, in 1988 and 1993, respectively. In 1993, the University of Valencia honored him with the Ph.D. Extraordinary Award. He is currently Full Professor of Optics at the University of Valencia, where he is co-leader of the "3D Imaging and Display Laboratory". His research interest includes resolution procedures in 3D scanning microscopy, and 3D imaging and display technologies. He has supervised on these topics seven Ph. D. theses, two of them honored with the Ph.D. Extraordinary Award. He has published over eighty technical articles in major journals, and pronounced over thirty invited and five keynote presentations in international meetings. He has been member of the Scientific Committee in over twenty international meetings. In 2010, Dr. Martinez-Corral was named Fellow of the SPIE. He is co-chair of the Three-Dimensional Imaging, Visualization, and Display Conference within the SPIE meeting in Defense, Security, and Sensing (Baltimore). He was Topical Editor of the IEEE/OSA JOURNAL OF DISPLAY TECHNOLOGY.